

SARS-CoV-2 Infection–Associated Hemophagocytic Lymphohistiocytosis

An Autopsy Series With Clinical and Laboratory Correlation

Andrey Prilutskiy, MD,^{1,*} Michael Kritselis, DO,¹ Artem Shevtsov, MD, PhD,¹ Ilyas Yambayev, MD,¹ Charitha Vadlamudi, MD,¹ Qing Zhao, MD, PhD,¹ Yachana Kataria, PhD,¹ Shayna R. Sarosiek, MD,² Adam Lerner, MD,² J. Mark Sloan, MD,² Karen Quillen, MD,² Eric J. Burks, MD¹

From the Departments of ¹Pathology and Laboratory Medicine and ²Hematology and Oncology, Boston University School of Medicine, Boston Medical Center, Boston, MA.

Key Words: SARS-CoV-2; Autopsy; Hemophagocytic lymphohistiocytosis; HLH; Coronavirus; Hemophagocytosis; 2019-nCoV; COVID-19

Am J Clin Pathol 2020;XX:0–0

DOI: 10.1093/AJCP/AQAA124

ABSTRACT

Objectives: *A subset of coronavirus disease 2019 (COVID-19) patients exhibit clinical features of cytokine storm. However, clinicopathologic features diagnostic of hemophagocytic lymphohistiocytosis (HLH) have not been reported. We studied the reticuloendothelial organs of 4 consecutive patients who died of COVID-19 and correlated with clinical and laboratory parameters to detect HLH.*

Methods: *Autopsies were performed on 4 patients who died of COVID-19. Routine H&E staining and immunohistochemical staining for CD163 were performed to detect hemophagocytosis. Clinical and laboratory results from premortem blood samples were used to calculate H-scores.*

Results: *All 4 cases demonstrated diffuse alveolar damage within the lungs. Three of the 4 cases had histologic evidence of hemophagocytosis within pulmonary lymph nodes. One case showed hemophagocytosis in the spleen but none showed hemophagocytosis in liver or bone marrow. Lymphohistiocytosis was the predominant form of hemophagocytosis observed. One patient showed diagnostic features of HLH with an H-score of 217, while a second patient likely had HLH with a partial H-score of 145 due to a missing triglyceride level. The remaining 2 patients had H-scores of 131 and 96.*

Conclusions: *This is the first report of severe acute respiratory syndrome coronavirus 2–associated HLH. Identification of HLH in a subset of patients with severe COVID-19 will inform clinical trials of therapeutic strategies.*

Key Points

- This is the first autopsy study specifically looking at the reticuloendothelial organs in fatal COVID-19.
- We observed 1 definite and 1 probable case of HLH out of 4 consecutive autopsy cases of SARS-CoV-2-associated ARDS with cytokine storm.
- The pathology community should be aware of possible secondary HLH in a subset of patients with severe COVID-19 to better manage COVID-19 patients experiencing cytokine storm.

The global pandemic of severe acute respiratory syndrome coronavirus 2 (SARS-CoV-2) has infected over 3.5 million people worldwide and has led to more than 250,000 deaths within just 5 months of the initial outbreak in Wuhan, China.¹ The rapid spread of the virus is largely the result of community transmission by individuals who are asymptomatic.² While some individuals remain asymptomatic throughout the disease course,³ others develop a flu-like illness with viral pneumonia that may progress to acute respiratory distress syndrome (ARDS), viral sepsis,⁴ and cytokine storm.⁵ The latter has raised clinical concerns for hemophagocytic lymphohistiocytosis (HLH) and the overlapping disorder, macrophage activation syndrome (MAS), highlighting the potential for therapeutic cytokine blockade.^{6–8}

Despite these clinical observations, there has been relatively little clinicopathologic correlation with the postmortem findings in COVID-19, which to date have generally focused on the pulmonary histology of diffuse alveolar damage.^{9–12} Herein we report the first cases of

SARS-CoV-2-associated HLH diagnosed postmortem using histologic, clinical, and laboratory criteria.

Materials and Methods

After obtaining consent from next of kin, autopsy was performed on 4 patients testing positive for SARS-CoV-2 nucleic acid on antemortem upper respiratory swab. Chart review of the electronic health record was performed to determine age, sex, race, date of symptom onset, date of hospitalization, date and types of treatment, CBC parameters, serum fibrinogen, ferritin, aspartate aminotransferase, and C-reactive protein (CRP). Laboratory values were obtained for each case on the day of intensive care unit transfer (average of hospital day 5 for patients 1, 3, and 4; hospital day 5 for patient 2). Ferritin levels were recorded over the entire hospital course. Triglyceride studies were performed on available antemortem blood samples after death in 3 of 4 patients.

The autopsies were performed in a negative pressure room using personal protective equipment including an N95 mask and powered air-purifying respirator. Autopsies were limited to chest and abdomen. Harvested organs were thinly sliced and fixed for 24 hours in 10% neutral-buffered formalin (NBF). Tissue blocks were prepared and fixed for an additional 6 to 12 hours in 10% NBF before processing. Bone marrow obtained by rib squeeze was fixed for 12 to 36 hours in B-Plus Fix (BBC Biochemical) fixative prior to processing without decalcification. H&E-stained sections were prepared and reviewed by 2 board-certified anatomic pathologists (E.J.B. and Q.Z.), one of whom is a board-certified hematopathologist (E.J.B.) with familiarity in evaluating samples for hemophagocytosis.

Immunohistochemistry and in situ hybridization were performed using freshly cut 5- μ m thick formalin-fixed paraffin-embedded tissue sections from lymph nodes, spleen, liver, and bone marrow. Slides were stained with CD163 clone MRQ-26 (Ventana, 760-4437), Pax-5 (Dako, DAK-Pax5), CD3 (Ventana, 2GV6), HHV-8 clone 13B10 (Leica, NCL-L-HHV8-LNA), CMV clone DDG9/CCH2 (Cell Marque, 213M-18), and EBER 1 DNP Probe (Ventana, 760-1209A) on a Ventana Benchmark Ultra (Ventana Medical Systems) after onboard heat-induced epitope retrieval with CC1 buffer (Ventana, 950-124) for immunohistochemistry or protease digestion for in situ hybridization. Slides were visualized with Optiview detection (Ventana, 760-700). Internal and external controls were examined for each slide and judged satisfactory before interpretation. As controls, spleen and mediastinal

lymph nodes from archived autopsies of 5 patients with non-COVID-19-related ARDS performed between 2007 and 2019 were stained with CD163. The presence of histiocytes phagocytosing nucleated cells was counted in 10 high power fields ($\times 200$ magnification) focusing on sinusoids, and the frequency of hemophagocytes containing single or multiple nucleated cells was calculated per 2 mm.²

H-scores were calculated based on clinical and laboratory data and using the presence of hemophagocytosis in one or more reticuloendothelial organs at autopsy to define the pathologic component of the score. The H-score is a validated tool that predicts HLH with 90% accuracy using a cutoff of 169.^{13,14}

The institutional review board reviewed this study and waived jurisdiction.

Results

Patient Characteristics and Treatment

Clinical features of the 4 patients are summarized in **Table 1**. They included 3 men and 1 woman, ranging from 64 to 91 years of age. Three were African American while 1 was white. Disease course included progressive hypoxia leading to intubation in 2 patients who died on day 15 and day 18 after symptom onset, while the remaining 2 patients were not intubated according to do not intubate orders. All patients received antibiotics during the hospital course including azithromycin, doxycycline, and/or ceftriaxone. Hydroxychloroquine was administered to two patients. Sarilumab, a human monoclonal antibody against the interleukin 6 receptor (IL-6R) was given to 2 patients, and anakinra, an interleukin-1 receptor (IL-1R) antagonist was given to 1 patient.

Autopsy Findings

The lungs showed acute exudative phase of diffuse alveolar damage in all 4 patients consistent with the clinical presentation of ARDS.

Mediastinal and pulmonary hilar lymph nodes were grossly enlarged and contained clusters of hemophagocytic histiocytes in 3 of 4 cases. In patient 1 this was characterized by a marked distention of cortical and subcortical sinuses with focal necrosis **Image 1A** and **Image 1B** as well as lymphocyte depletion. In patients 2 and 3 the finding was more limited, with multifocal clusters of hemophagocytic histiocytes localizing in the subcapsular sinuses **Image 1C** and

Table 1
Clinicopathologic Features

	Patient 1	Patient 2	Patient 3	Patient 4
Age, y	72	91	72	64
Sex	M	M	M	F
Race	W	AA	AA	AA
Symptom onset until				
Hospitalization, d	4	1	3	5
Treatment, d	d 5: HCQ/AZI d 6-8: Anakinra d 7: Intubation	d 1: HCQ/DOX/AZI	d 3: CRO/AZI d 4: Sarilumab	d 5: Sarilumab d 6: CRO d 12: Intubation
Death, d	18	8	6	15
Highest body temperature (°C)	40	38.9	38.3	38.8
WBC count, × 10 ³ /μL	6.2	10.6	11.1	9.8
Absolute lymphocyte count, × 10 ³ /μL	0.6	0.8	0.8	1.2
Hemoglobin, g/dL	10.2	8.9	10.5	14.6
Platelet count, × 10 ³ /μL	108	317	681	261
Fibrinogen, mg/dL	418	800	800	559
Ferritin, ng/mL	7,679	4,095	167	397
Triglyceride, mg/dL	1,316	—	162	353
Aspartate transaminase, U/L	63	37	59	32
C-reactive protein, mg/L	81.6	354.6	365.1	77.7
Hepatomegaly	No	No	No	No
Splenomegaly	No	Yes	No	No
Hemophagocytosis				
Lymph node	Yes	Yes	Yes	No
Spleen	No	Yes	No	No
Liver	No	No	No	No
Bone marrow	—	—	No	No
H-score	217	145 ^a	131	96
HLH syndrome	Definite	Probable	Absent	Absent

AA, African American; AZI, azithromycin; DOX, doxycycline; CRO, ceftriaxone; HCQ, hydroxychloroquine; HLH, hemophagocytic lymphohistiocytosis; W, white.

^aPartial H-score as triglyceride level was not available for this patient. Laboratory values were obtained for each case on the day of intensive care unit transfer (average of hospital day 5 for patients 1, 3, and 4; hospital day 5 for patient 2).

Image 1D. Lymphoid depletion was not identified in these cases; follicular and interfollicular hyperplasia was present in patient 3. Lymphophagocytosis was the predominant form of hemophagocytosis in all patients **Image 1E**, with frequent occurrence of multiple lymphocytes engulfed within single histiocytes most easily visualized using CD163 immunohistochemical stain **Image 1F**. Representative images of lymph nodes with and without lymphoid depletion using H&E and immunohistochemical stains for Pax-5 and CD3 are shown in **Supplemental Image 1** (all supplemental materials can be found at *American Journal of Clinical Pathology* online). Immunohistochemistry for human herpesvirus-8 (HHV-8), cytomegalovirus (CMV), and Epstein-Barr virus (EBV) by in situ hybridization for EBV small RNA (EBER) were negative in lymph nodes with hemophagocytosis. As controls, mediastinal lymph nodes from autopsies of 5 patients with non-COVID-19-related ARDS were stained with CD163 and only rare lymphophagocytic histiocytes were observed (range, 0-0.6 per 2 mm²), and no histocytes containing multiple lymphocytes were seen.

The spleen was enlarged in a single patient (patient 2) with a soft and friable gross appearance that ruptured on evisceration. Microscopically there were numerous areas of red pulp hemorrhage with admixed phagocytic histiocytes, focally showing hemophagocytosis **Image 2A**, **Image 2B**, and **Image 2C** and white pulp depletion. Spleen size was normal in the remaining patients. In patient 1 there was white pulp depletion with red pulp infarction **Image 2D**, histiocytic hyperplasia **Image 2E**, and numerous hemosiderin-laden macrophages suggestive of prior RBC phagocytosis **Image 2F**. In patients 3 and 4, the spleens showed normal to slightly hyperplastic white pulp with red pulp congestion but lacking hemophagocytosis. As controls, sections of spleen from autopsies of 5 patients with non-COVID-19-related ARDS were stained with CD163, and only rare lymphophagocytic histiocytes were observed (range, 0-0.6 per 2 mm²), and no histocytes containing multiple lymphocytes were seen.

The liver was not enlarged in any of the patients. Histologically there was mild centrilobular congestion with mild steatosis in a subset of cases but without significant portal or lobular inflammation. Minimal

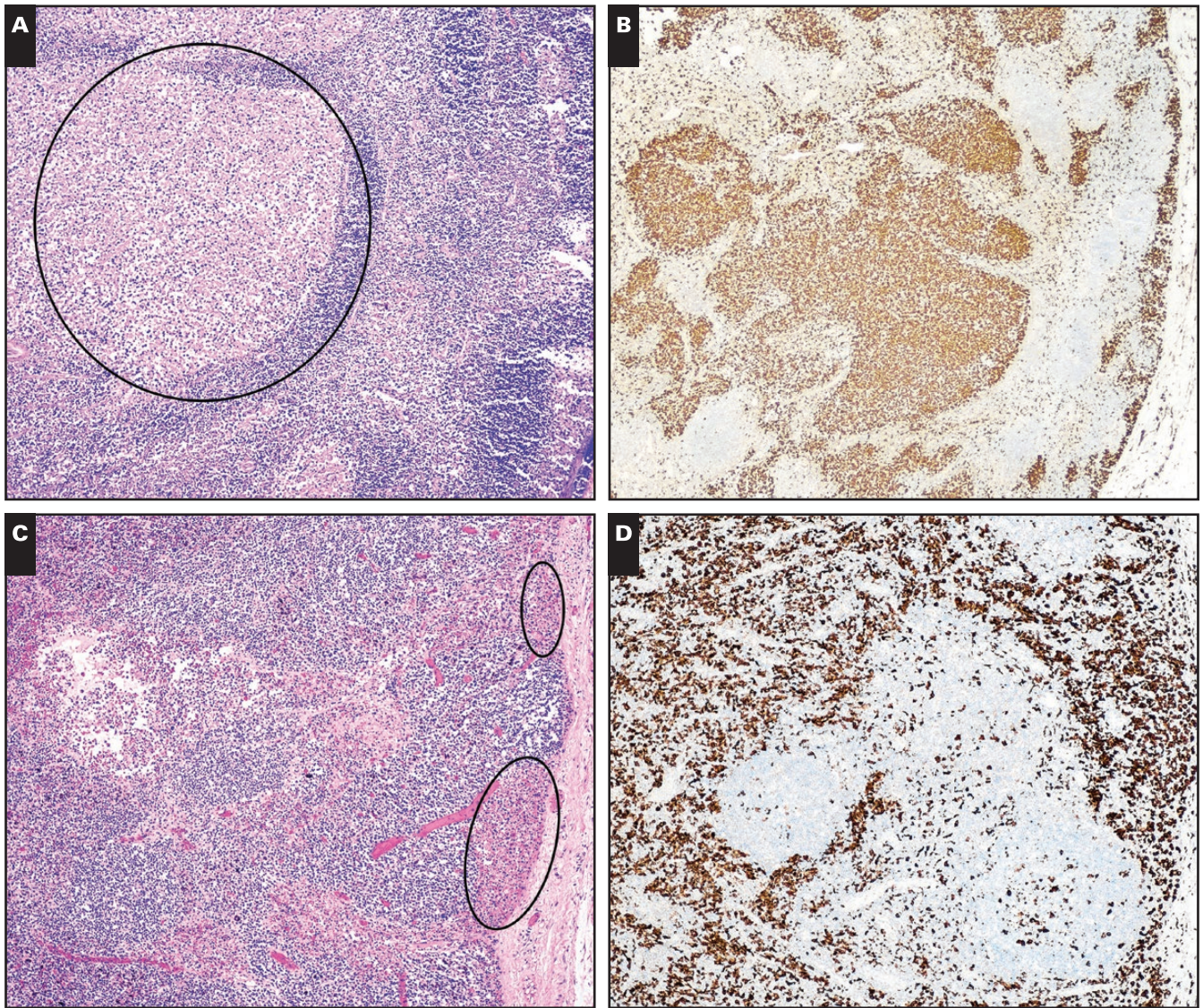


Image 1 Hemophagocytosis in pulmonary hilar and mediastinal lymph nodes. H&E (A) and CD163 immunohistochemical (B) stains of lymph node from patient 1 showing distended cortical and subcortical sinusoids filled with histiocytes exhibiting focal necrosis (circled area). (×40). H&E (C) and CD163 immunohistochemical (D) stains of a lymph node from patient 2 showing a lesser degree of sinusoidal expansion, predominantly filling the subcapsular sinuses (circled areas) (×40).

Kupffer cell hyperplasia was seen on CD163 staining, but hemophagocytosis was not observed **Image 3**.

Bone marrow particles were examined on patients 3 and 4, and these showed trilineage hematopoiesis with left-shifted myeloid hyperplasia. Immunohistochemistry for CD163 showed a mild histiocytic hyperplasia but no hemophagocytosis.

Clinicopathologic Correlation

The presence of hemophagocytosis detected at autopsy was used in conjunction with laboratory findings from premortem laboratory specimens to calculate

H-scores (Table 1). Patient 1 had an H-score of 217, meeting the clinicopathologic definition of HLH, with extensive hemophagocytosis despite treatment with anakinra. Patient 2 had a partial H-score of 145, as the triglyceride level was not available. Given the hemophagocytosis in lymph nodes and enlarged spleen, and progressive rise in ferritin level, we believe this patient likely had HLH. Patient 3 had focal subcapsular hemophagocytosis in a mediastinal lymph node but did not exhibit clinical criteria of HLH (H-score of 131). Patient 4, who did not show hemophagocytosis in any reticuloendothelial organ, had the lowest H-score of 96. Of note, no patient in our series exhibited hypofibrinogenemia or bicytopenia/pancytopenia. **Figure 1** shows the rate of

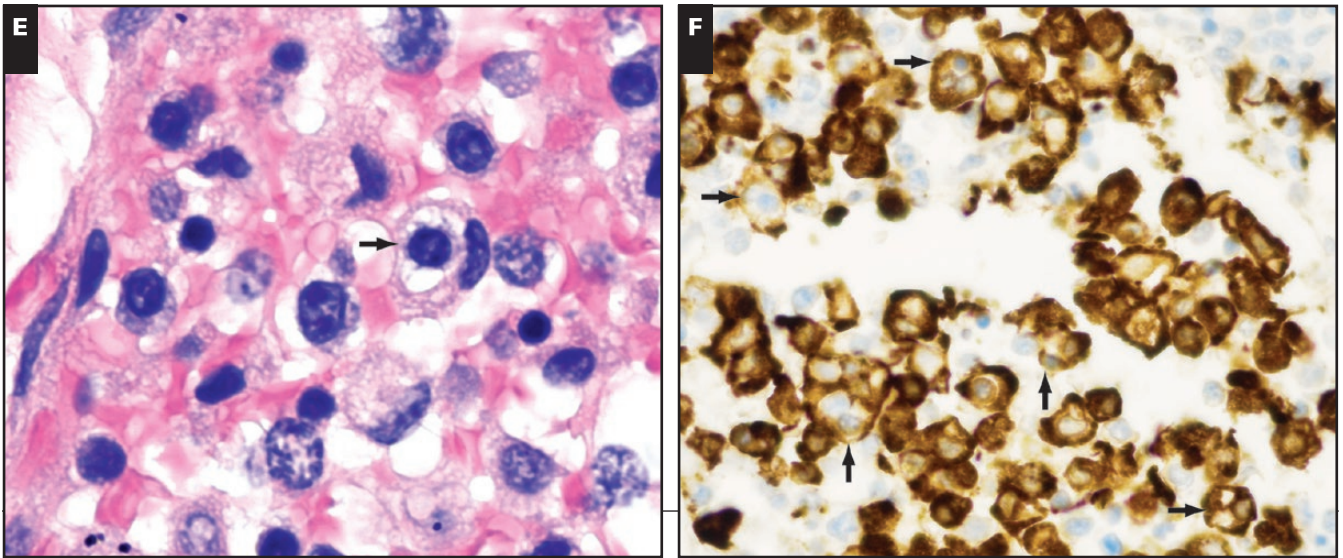


Image 1 (cont) Hemophagocytosis consisted predominantly of lymphophagocytosis (arrow) in all cases and seen on H&E stain (**E**, $\times 1,000$) and highlighted with CD163 immunohistochemical stain where numerous histiocytes phagocytosing 1 to several lymphocytes were apparent (arrows) (**F**, $\times 400$).

ferritin rise in each of the 4 patients. Patient 1 and 2 with definite and probable HLH exhibited progressive rise in ferritin levels beginning early in the disease course. Ferritin levels were low throughout most of the disease course of patients 3 and 4, although both received sarilumab early in admission. There was a late rise in ferritin level in patient 4 likely reflecting tissue injury resulting from multiple thromboemboli causing pulmonary embolism and stroke the day preceding death. All patients showed elevation of CRP levels.

Discussion

To date in the pandemic, only a limited number of scientific publications on the histopathologic findings in patients with COVID-19 are available. Most have focused on pulmonary findings either from resections for lung cancer or postmortem tissue biopsy of lung, heart, and liver.⁹⁻¹² Given the reports of a subset of patients exhibiting clinical features of cytokine storm,⁵ we studied our first 4 autopsies of COVID-19 patients for histologic evidence of hemophagocytosis within the reticuloendothelial organs (lymph node, spleen, bone marrow, and liver) and correlated with clinical and laboratory parameters to detect the syndrome of HLH. We observed 1 patient with definite HLH and 1 with probable HLH of the 4 patients studied.

HLH in adults is a rare life-threatening disease associated with infection, neoplasms, and autoimmune disease.¹⁵ In the latter situation MAS is frequently applied as a subtype of HLH.¹⁶ Defective granule-mediated

cytotoxicity is implicated as the pathophysiologic mechanism resulting in dysregulated antigen presentation and leading to excessive secretion of proinflammatory cytokines referred to as “cytokine storm.” In children this is often related to autosomal recessive mutations in the NK/T-cell cytotoxic pathway termed primary/familial HLH.¹⁷ Secondary HLH (sHLH), also called reactive HLH, can present at any age but frequently occurs in patients with underlying diseases affecting immunity including HIV and cancer.¹⁸

The diagnosis of HLH is based on a constellation of clinical, laboratory, and morphologic criteria.¹⁹ The H-score is a clinical tool that estimates the probability of HLH based on severity of fever; hepatosplenomegaly; number of cytopenias; elevations in serum ferritin, triglyceride, aspartate aminotransferase levels; hypofibrinogenemia; and morphologic presence of hemophagocytosis.^{13,14} In a larger cohort of 191 inpatients with COVID-19 in Wuhan, China, nonsurvivors compared to survivors more frequently had anemia (26% vs 11%), thrombocytopenia (20% vs 1%), and elevated alanine aminotransferase (48% vs 24%) and ferritin levels (96% vs 71%).²⁰ In particular, ferritin levels of 2,000 ng/mL or greater were observed in 25% of fatal cases. Alternatively, leukopenia showed the opposite trend, being observed in 9% of nonsurvivors vs 20% of survivors. The frequency of organomegaly, hypofibrinogenemia, or hypertriglyceridemia is currently not known for COVID-19. In our series, high fever, hyperferritinemia, and hypertriglyceridemia were the most helpful clinical and laboratory finding distinguishing HLH from non-HLH

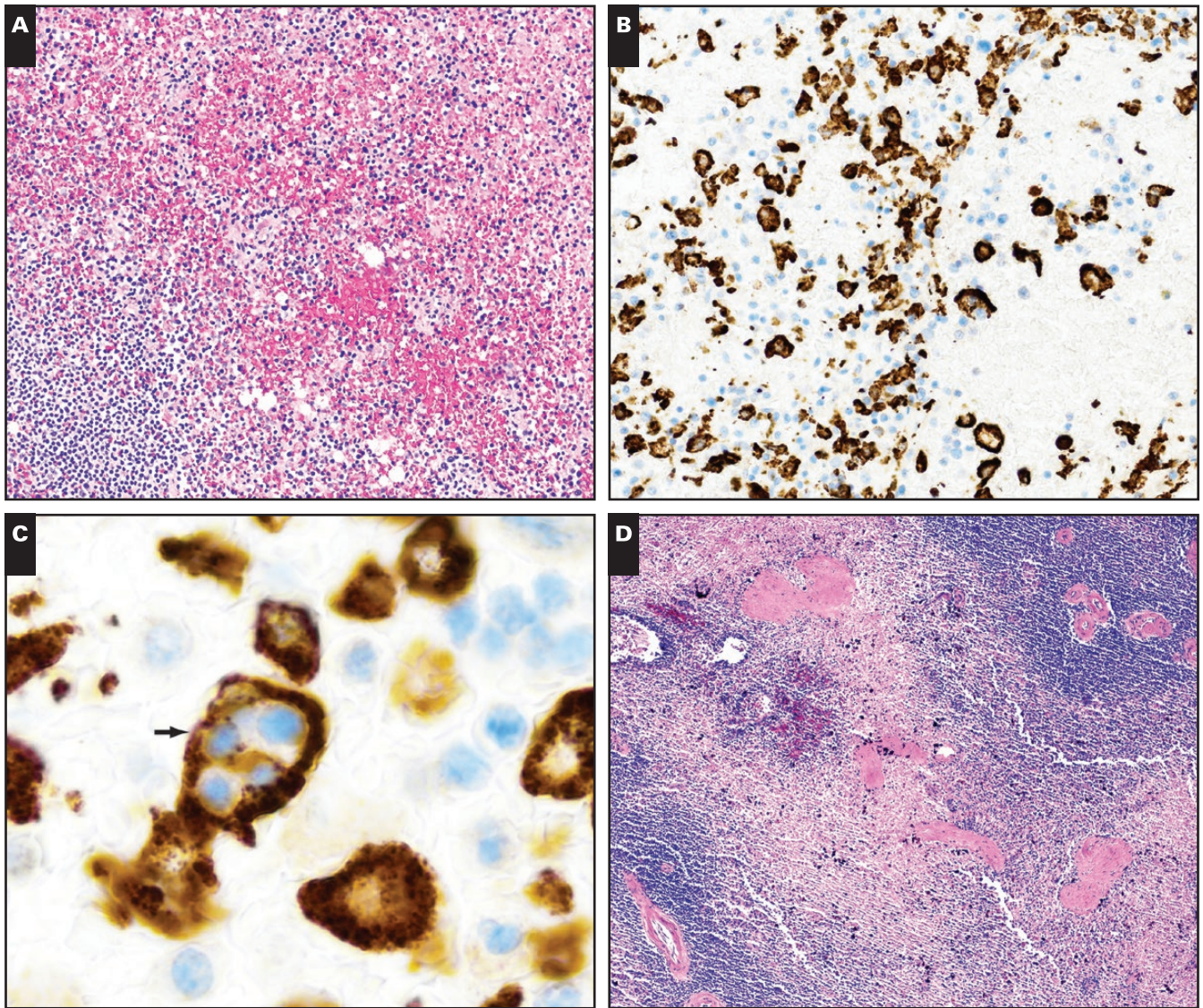


Image 2 Hemophagocytosis in spleen. H&E stain of spleen from patient 2 with white pulp depletion and red pulp hemorrhage (**A**, $\times 100$) with CD163 immunohistochemical stain demonstrating mild histiocytic hyperplasia (**B**, $\times 100$) and lymphophagocytosis (arrow) (**C**, $\times 1,000$). H&E stain of spleen from patient 1 showing mild white pulp depletion and red pulp infarction (**D**, $\times 40$).

COVID-19 patients with ARDS. Elevated CRP levels were noted in all 4 cases, consistent with the cytokine storm that is prevalent in severe COVID-19 infections.⁴ We observed no patient with bicytopenia, pancytopenia, or hypofibrinogenemia, as is often seen in other infection-associated HLH, but larger studies are required to further characterize whether this is a unique feature of SARS-CoV-2-associated HLH.

Pathologic detection of hemophagocytosis is 1 criterion used in the diagnosis of HLH. Bone marrow biopsies are the typical antemortem specimen; however, lymph nodes also exhibit characteristic pathologic features.²¹ Some have questioned the specificity of hemophagocytosis,

as it has also been observed in 64.5% of bone marrow aspirates in patients with sepsis²² and rarely within normal bone marrow biopsies.^{23,24} This may be in part explained by the variable definitions of the hemophagocyte, specifically regarding the engulfment of anucleate cells such as erythrocytes and platelets compared to phagocytosis of nucleated cells such as neutrophils, RBC precursors, and lymphocytes. Detailed pathologic studies of bone marrow biopsies in this regard have shown that nucleated cell phagocytosis as well as multiply phagocytosed nucleated cells within single macrophages have higher specificity for the diagnosis of HLH than erythrophagocytosis alone.²⁵ Our observation of a high density of macrophages engulfing

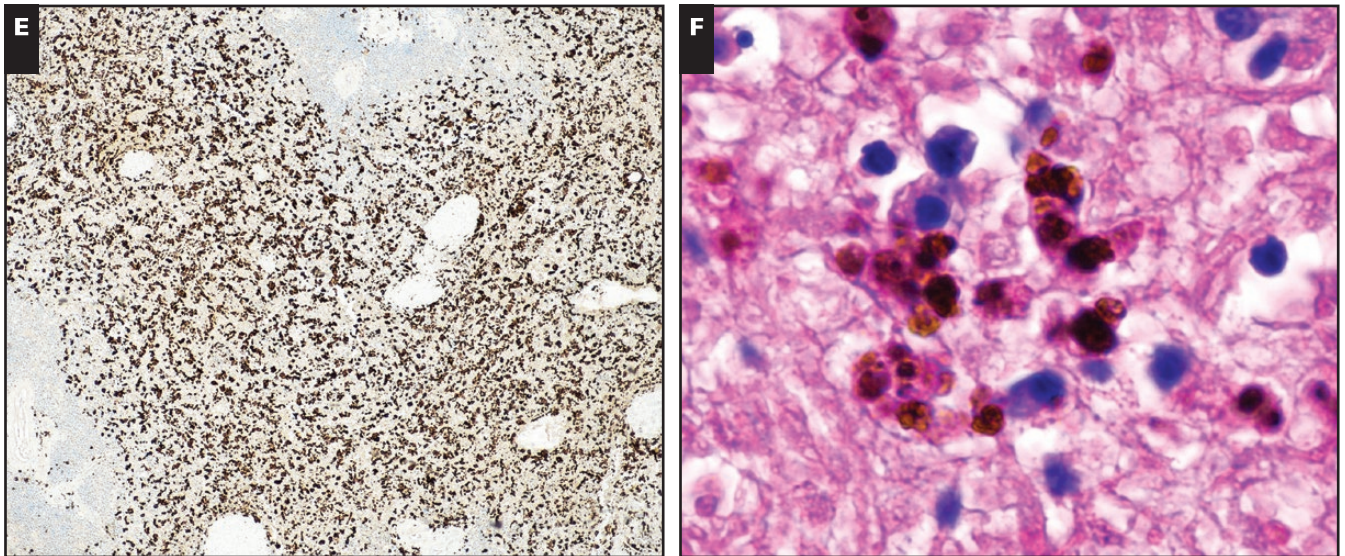


Image 2 (cont) CD163 immunohistochemical stain showing moderate histiocytic hyperplasia (**E**, $\times 40$) and hemosiderin-laden macrophages suggestive of prior erythrophagocytosis (**F**, $\times 1,000$).

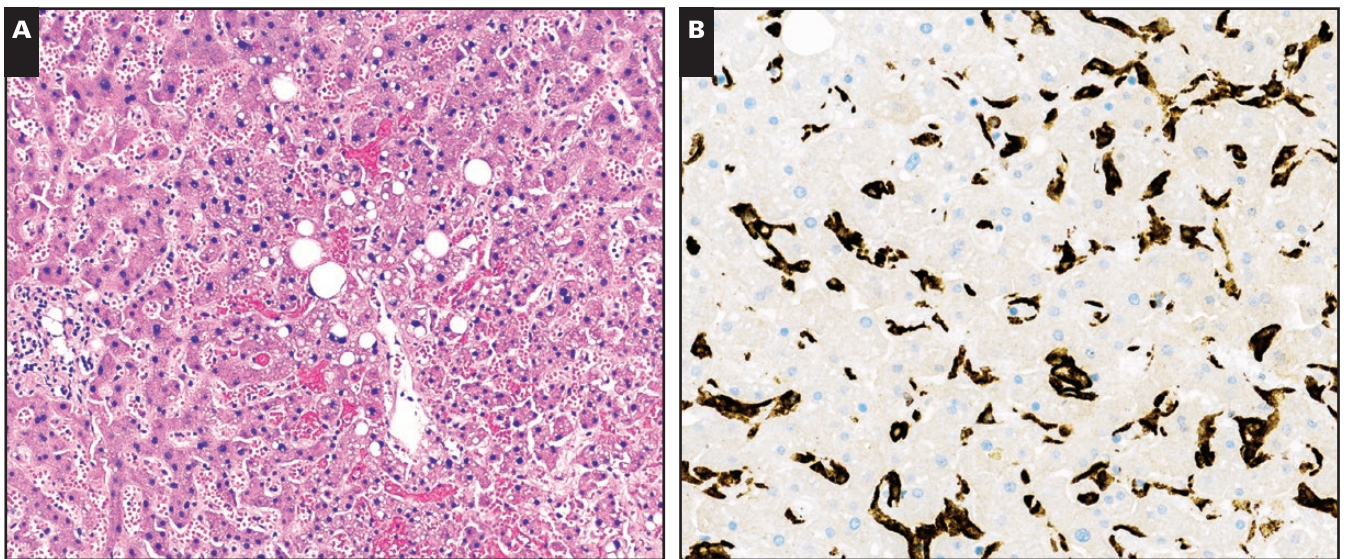


Image 3 Liver without hemophagocytosis. **A**, H&E stain of liver showing mild centrilobular congestion with mild steatosis ($\times 200$). **B**, CD163 immunohistochemical stain showing mild Kupffer cell hyperplasia without hemophagocytosis ($\times 200$).

multiple lymphocytes thus warrants greater consideration than erythrophagocytosis, which is observed in a variety of disease states.

Infection-associated sHLH is most often caused by DNA viruses of the Herpesviridae family—EBV, CMV, and Kaposi sarcoma–associated virus (HHV-8)¹⁵—which were excluded in our cases. RNA viruses have also been implicated as triggering agents of sHLH, particularly in the epidemic or pandemic setting. In this context, HLH has been observed in a subset of fatal infections

with SARS-CoV-1,²⁶⁻³⁰ novel avian-origin influenza A (H5N1),³¹⁻³³ and swine-origin influenza A (H1N1).^{34,35} Intriguingly, among a cohort of 16 fatal H1N1 adult patients, 81% exhibited hemophagocytosis at autopsy and 36% were retrospectively found to harbor heterozygous mutations in familial HLH-associated genes using whole-exome sequencing.³⁶ Similarly, others have reported that 14% of sporadic adult onset HLH harbor hypomorphic mutations in familial HLH-associated genes.³⁷ Taken together, these data may explain why a subset of patients

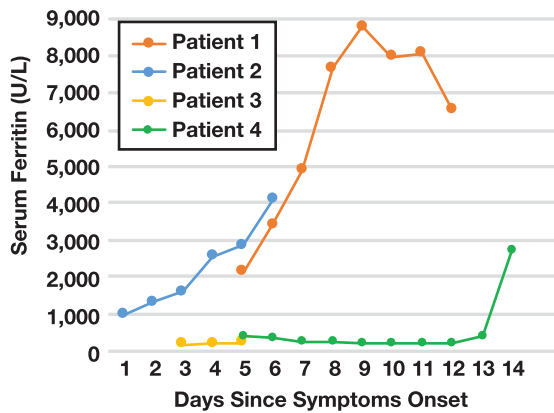


Figure 1 Serum ferritin levels over disease course.

in pandemic settings exhibit a hyperinflammatory disease course characterized by HLH with cytokine storm. This concept has recently been reviewed and presented as a threshold model for MAS/sHLH.³⁸ Prospective molecular studies interrogating these immune abnormalities in individuals with COVID-19 may be useful in predicting which individuals are at greatest risk of cytokine storm.

Herein we report the first documented cases of HLH associated with SARS-CoV-2 in patients whose clinical courses were dominated by ARDS and cytokine storm. High fever, hyperferritinemia, and hypertriglyceridemia were the most useful clinical parameters to identify HLH among our COVID-19 autopsy cohort. Recognition of cytokine storm as a manifestation of sHLH is critical to ensure timely anti-inflammatory treatment concurrent with antiviral therapy in patients with COVID-19.^{5,6} We note that an etoposide-based regimen, typically used to treat EBV-associated HLH, has been used to successfully treat a patient with H1N1-associated HLH who was receiving extracorporeal membrane oxygenation.³⁹ In addition, a variety of targeted approaches against inflammatory cytokines traditionally used in the setting of autoimmune disease-associated MAS have been proposed.^{7,8} Of note, patient 1, who had definitive SARS-CoV-2-associated HLH in our cohort, received anakinra (IL-1R antagonist) with persistence of hemophagocytosis at autopsy. Hemophagocytosis but not HLH was seen in 1 of 2 patients who received sarilumab (anti-IL-6R mAb). Clinicians should be aware of the signs and laboratory features of HLH, which may develop in a subset of SARS-CoV-2 infections. Identification of the hyperinflammatory clinical phenotype will inform

clinical trials of optimal therapy in this life-threatening condition.

Corresponding author: Eric J. Burks, MD; ejburks@bu.edu.

Acknowledgments: We acknowledge the technical assistance of Teresa Lima, Emily Aniskovich, Myrtha Constant, and Cheryl Spencer.

Funding was partially provided by the Boston University Mallory Pathology Associates and Boston Medical Center.

References

1. Johns Hopkins Coronavirus Resource Center. COVID-19 map. <https://coronavirus.jhu.edu/map.html>. Accessed May 4, 2020.
2. Arons MM, Hatfield KM, Reddy SC, et al. Presymptomatic SARS-CoV-2 infections and transmission in a skilled nursing facility. *N Engl J Med*. 2020. doi:10.1056/NEJMoa2008457.
3. Pan Y, Yu X, Du X, et al. Epidemiological and clinical characteristics of 26 asymptomatic SARS-CoV-2 carriers. *J Infect Dis*. 2020. doi:10.1093/infdis/jiaa205.
4. Li H, Liu L, Zhang D, et al. SARS-CoV-2 and viral sepsis: observations and hypotheses. *Lancet*. 2020;395:1517-1520. doi:10.1016/S0140-6736(20)30920-X.
5. Mehta P, McAuley DF, Brown M, et al. COVID-19: consider cytokine storm syndromes and immunosuppression. *Lancet*. 2020;395:1033-1034. doi:10.1016/S0140-6736(20)30628-0.
6. McGonagle D, Sharif K, O'Regan A, et al. The role of cytokines including interleukin-6 in COVID-19 induced pneumonia and macrophage activation syndrome-like disease. *Autoimmun Rev*. 2020;19:102537. doi:10.1016/j.autrev.2020.102537.
7. Cron RQ, Chatham WW. The rheumatologist's role in COVID-19. *J Rheumatol*. 2020. doi:10.3899/jrheum.200334.
8. Misra DP, Agarwal V, Gasparyan AY, et al. Rheumatologists' perspective on coronavirus disease 19 (COVID-19) and potential therapeutic targets. *Clin Rheumatol*. 2020. doi:10.1007/s10067-020-05073-9.
9. Carsana L, Sonzogni A, Nasr A, et al. Pulmonary post-mortem findings in a large series of COVID-19 cases from Northern Italy. *Infect Dis*. 2020. doi:10.1101/2020.04.19.20054262.
10. Tian S, Hu W, Niu L, et al. Pulmonary pathology of early-phase 2019 novel coronavirus (COVID-19) pneumonia in two patients with lung cancer. *J Thorac Oncol*. 2020;15:700-704. doi:10.1016/j.jtho.2020.02.010.
11. Tian S, Xiong Y, Liu H, et al. Pathological study of the 2019 novel coronavirus disease (COVID-19) through post-mortem core biopsies. *Mod Pathol*. 2020. doi:10.1038/s41379-020-0536-x.
12. Xu Z, Shi L, Wang Y, et al. Pathological findings of COVID-19 associated with acute respiratory distress syndrome. *Lancet Respir Med*. 2020;8:420-422. doi:10.1016/S2213-2600(20)30076-X.
13. Debaugnies F, Mahadeb B, Ferster A, et al. Performances of the H-score for diagnosis of hemophagocytic lymphohistiocytosis in adult and pediatric patients. *Am J Clin Pathol*. 2016;145:862-870. doi:10.1093/ajcp/aqw076.

14. Fardet L, Galicier L, Lambotte O, et al. Development and validation of the Hscore, a score for the diagnosis of reactive hemophagocytic syndrome. *Arthritis Rheumatol*. 2014;66:2613-2620. doi:10.1002/art.38690.
15. Ramos-Casals M, Brito-Zerón P, López-Guillermo A, et al. Adult haemophagocytic syndrome. *Lancet*. 2014;383:1503-1516. doi:10.1016/S0140-6736(13)61048-X.
16. Grom AA, Horne A, De Benedetti F. Macrophage activation syndrome in the era of biologic therapy. *Nat Rev Rheumatol*. 2016;12:259-268. doi:10.1038/nrrheum.2015.179.
17. Rosado FGN, Kim AS. Hemophagocytic lymphohistiocytosis: an update on diagnosis and pathogenesis. *Am J Clin Pathol*. 2013;139:713-727. doi:10.1309/AJCP4ZDKJ4ICOUAT.
18. Gupta S, Weitzman S. Primary and secondary hemophagocytic lymphohistiocytosis: clinical features, pathogenesis and therapy. *Expert Rev Clin Immunol*. 2010;6:137-154. doi:10.1586/eci.09.58.
19. Bergsten E, Horne A, Aricó M, et al. Confirmed efficacy of etoposide and dexamethasone in HLH treatment: long-term results of the cooperative HLH-2004 study. *Blood*. 2017;130:2728-2738. doi:10.1182/blood-2017-06-788349.
20. Zhou F, Yu T, Du R, et al. Clinical course and risk factors for mortality of adult inpatients with COVID-19 in Wuhan, China: a retrospective cohort study. *Lancet*. 2020;395:1054-1062. doi:10.1016/S0140-6736(20)30566-3.
21. Risdall RJ, McKenna RW, Nesbit ME, et al. Virus-associated hemophagocytic syndrome: a benign histiocytic proliferation distinct from malignant histiocytosis. *Cancer*. 1979;44:993-1002. doi:10.1002/1097-0142(197909)44:3<993::AID-CNCR2820440329>3.0.CO;2-5.
22. Strauss R, Neureiter D, Westenburger B, et al. Multifactorial risk analysis of bone marrow histiocytic hyperplasia with hemophagocytosis in critically ill medical patients—a postmortem clinicopathologic analysis. *Crit Care Med*. 2004;32:1316-1321. doi:10.1097/01.CCM.0000127779.24232.15.
23. Goel S, Polski JM, Imran H. Sensitivity and specificity of bone marrow hemophagocytosis in hemophagocytic lymphohistiocytosis. *Ann Clin Lab Sci*. 2012;42:21-25.
24. Gupta A, Weitzman S, Abdelhaleem M. The role of hemophagocytosis in bone marrow aspirates in the diagnosis of hemophagocytic lymphohistiocytosis. *Pediatr Blood Cancer*. 2008;50:192-194. doi:10.1002/pbc.21441.
25. Gars E, Purington N, Scott G, et al. Bone marrow histomorphological criteria can accurately diagnose hemophagocytic lymphohistiocytosis. *Haematologica*. 2018;103:1635-1641. doi:10.3324/haematol.2017.186627.
26. Gu J, Korteweg C. Pathology and pathogenesis of severe acute respiratory syndrome. *Am J Pathol*. 2007;170:1136-1147. doi:10.2353/ajpath.2007.061088.
27. Wong RSM, Wu A, To KF, et al. Haematological manifestations in patients with severe acute respiratory syndrome: retrospective analysis. *BMJ*. 2003;326:1358-1362. doi:10.1136/bmj.326.7403.1358.
28. Chong PY, Chui P, Ling AE, et al. Analysis of deaths during the severe acute respiratory syndrome (SARS) epidemic in Singapore: challenges in determining a SARS diagnosis. *Arch Pathol Lab Med*. 2004;128:195-204. doi:10.1043/1543-2165(2004)128<195:AODDTS>2.0.CO;2.
29. Lang Z-W, Zhang L-J, Zhang S-J, et al. A clinicopathological study of three cases of severe acute respiratory syndrome (SARS). *Pathology (Phila)*. 2003;35:526-531. doi:10.1080/00313020310001619118.
30. Nicholls JM, Poon LLM, Lee KC, et al. Lung pathology of fatal severe acute respiratory syndrome. *Lancet*. 2003;361:1773-1778. doi:10.1016/S0140-6736(03)13413-7.
31. Yuen KY, Chan PK, Peiris M, et al. Clinical features and rapid viral diagnosis of human disease associated with avian influenza A H5N1 virus. *Lancet*. 1998;351:467-471. doi:10.1016/S0140-6736(98)01182-9.
32. Cheung CY, Poon LLM, Lau AS, et al. Induction of proinflammatory cytokines in human macrophages by influenza A (H5N1) viruses: a mechanism for the unusual severity of human disease? *Lancet*. 2002;360:1831-1837. doi:10.1016/S0140-6736(02)11772-7.
33. To KF, Chan PK, Chan KF, et al. Pathology of fatal human infection associated with avian influenza A H5N1 virus. *J Med Virol*. 2001;63:242-246. doi:10.1002/1096-9071(200103)63:3<242::aid-jmv1007>3.0.co;2-n.
34. Harms PW, Schmidt LA, Smith LB, et al. Autopsy findings in eight patients with fatal H1N1 influenza. *Am J Clin Pathol*. 2010;134:27-35. doi:10.1309/AJCP35KOZSAVNQZW.
35. Soto-Abraham MV, Soriano-Rosas J, Díaz-Quinónez A, et al. Pathological changes associated with the 2009 H1N1 virus. *N Engl J Med*. 2009;361:2001-2003. doi:10.1056/NEJMc0907171.
36. Schulert GS, Zhang M, Fall N, et al. Whole-exome sequencing reveals mutations in genes linked to hemophagocytic lymphohistiocytosis and macrophage activation syndrome in fatal cases of H1N1 influenza. *J Infect Dis*. 2016;213:1180-1188. doi:10.1093/infdis/jiv550.
37. Zhang K, Jordan MB, Marsh RA, et al. Hypomorphic mutations in PRF1, MUNC13-4, and STXBP2 are associated with adult-onset familial HLH. *Blood*. 2011;118:5794-5798. doi:10.1182/blood-2011-07-370148.
38. Schulert GS, Cron RQ. The genetics of macrophage activation syndrome. *Genes Immun*. 2020. doi:10.1038/s41435-020-0098-4.
39. Henter JI, Palmkvist-Kaijser K, Holzgraefe B, et al. Cytotoxic therapy for severe swine flu A/H1N1. *Lancet*. 2010;376:2116. doi:10.1016/S0140-6736(10)61345-1.